Schizophrenia Bulletin vol. 43 no. 6 pp. 1363–1374, 2017
doi:10.1093/schbul/sbx051
Advance Access publication May 17, 2017

Altered Coupling Between Resting-State Cerebral Blood Flow and Functional Connectivity in Schizophrenia

Jiajia Zhu[1], Chuanjun Zhuo[1–3], Lixue Xu[1], Feng Liu[1], Wen Qin[1], and Chunshui Yu[*,1]

[1]Department of Radiology and Tianjin Key Laboratory of Functional Imaging, Tianjin Medical University General Hospital, Tianjin, China; [2]Department of Psychiatry Functional Neuroimaging Laboratory, Tianjin Mental Health Center, Tianjin Anding Hospital, Tianjin, China; [3]Tianjin Anning Hospital, Tianjin, China

*To whom correspondence should be addressed; Department of Radiology, Tianjin Medical University General Hospital, No. 154, Anshan Road, Heping District, Tianjin 300052, China; tel: +86-22-63062026, fax: +86-22-63062290, e-mail: chunshuiyu@tijmu.edu.cn

Background: **Respective changes in resting-state cerebral blood flow (CBF) and functional connectivity in schizophrenia have been reported. However, their coupling alterations in schizophrenia remain largely unknown.** ***Methods:*** **89 schizophrenia patients and 90 sex- and age-matched healthy controls underwent resting-state functional MRI to calculate functional connectivity strength (FCS) and arterial spin labeling imaging to compute CBF. The CBF-FCS coupling of the whole gray matter and the CBF/FCS ratio (the amount of blood supply per unit of connectivity strength) of each voxel were compared between the 2 groups.** ***Results:*** **Whole gray matter CBF-FCS coupling was decreased in schizophrenia patients relative to healthy controls. In schizophrenia patients, the decreased CBF/FCS ratio was predominantly located in cognitive- and emotional-related brain regions, including the dorsolateral prefrontal cortex, insula, hippocampus and thalamus, whereas an increased CBF/FCS ratio was mainly identified in the sensorimotor regions, including the putamen, and sensorimotor, mid-cingulate and visual cortices.** ***Conclusion:*** **These findings suggest that the neurovascular decoupling in the brain may be a possible neuropathological mechanism of schizophrenia.**

Key words: arterial spin labeling/cerebral blood flow/functional magnetic resonance imaging/functional connectivity/resting-state/schizophrenia

Introduction

Schizophrenia is a devastating illness with unknown etiology and has a prevalence of approximately 1% in the general population.[1] In recent decades, neuroimaging techniques have provided evidence for the dysconnectivity hypothesis, which links schizophrenia to disrupted structural and functional connections in the brain.[2–4] Using functional MRI (fMRI), resting-state functional connectivity (rsFC) that measures the temporal correlations of low-frequency fluctuations in the blood-oxygen-level-dependent (BOLD) signal across brain regions, has been proposed to reflect the intrinsic functional organization of the brain.[5,6] Seed-based rsFC analysis, independent component analysis (ICA) and graph theory-based analysis have been used to quantify rsFC alterations in schizophrenia and have revealed extensive functional dysconnectivity,[7] including dysconnectivity of the specific regions (eg, the prefrontal cortex), circuits (eg, the cortical-subcortical circuit), subnetworks (eg, the default mode network and salience network), and the whole brain network.[8]

The seed-based rsFC method is widely used because of its inherent simplicity, sensitivity and ease of interpretation.[6] However, this method needs a priori definition of seed regions; thus, the analysis may be difficult if the underlying pathology for a disease is unknown.[9] This problem is partially overcome by the ICA approach, which automatically separates the signals of the whole brain into statistically independent components, resulting in spatially non-overlapping functional subnetworks.[10,11] However, the ICA may encounter uncertainty regarding the most appropriate number of components, controversial criteria for distinguishing between noise and signal, and interpretive complexities introduced by a sophisticated algorithm.[6] The whole-brain functional connectivity strength (FCS) analysis is a newly developed data-driven method to test the connectivity of each voxel with all other voxels in the brain.[12–14] The FCS is also referred to as the "degree centrality" of weighted networks in graph theory,[12–15] and brain regions with high FCS are considered functional hubs that are highly connected to the rest of the brain. The FCS approach has been applied to investigate connectivity changes in

schizophrenia and has revealed increased or reduced FCS in the prefrontal regions and decreased FCS in the sensorimotor and visual cortices (supplementary table S1).[16–19]

Cerebral blood flow (CBF) is defined as the volume of blood delivered to a given mass of brain tissue over a given time. Resting-state CBF is closely coupled with brain metabolism, including glucose utilization, oxygen consumption, and aerobic glycolysis.[20,21] Positron emission tomography (PET) and single photon emission computerized tomography (SPECT) have been extensively used to identify CBF deficits in schizophrenia. Using these techniques, many previous studies have demonstrated that schizophrenia patients exhibited an increased or decreased resting-state CBF in multiple brain regions, especially a decreased CBF in the prefrontal cortex.[22–30] However, both techniques are invasive, with a long acquisition time and low spatial resolution. In contrast, the arterial spin labeling (ASL) MRI is a noninvasive technique that can rapidly quantify CBF using an endogenous contrast.[31,32] This technique has been used to explore CBF alterations in schizophrenia and has demonstrated increased CBF in the striatum, decreased CBF in the prefrontal and anterior cingulate cortices, and increased or reduced CBF in the thalamus and temporal cortex (supplementary table S2).[33–37]

Nearly 20% energy is consumed by the human brain, which is 10 times higher than what would be expected from its relative size to the body.[38,39] Most of the energy is consumed to support spontaneous brain activity.[40] Based on the neurovascular coupling hypothesis, brain regions with stronger connectivity tend to have higher spontaneous neuronal activity with greater metabolic demand, resulting in increased perfusion.[41,42] As expected, a higher degree of functional connectivity is associated with increases in glucose metabolism (energy consumption) in healthy subjects.[43] Moreover, several studies have identified an association between CBF and brain connectivity. For example, network analyses have found correlations between CBF and anatomical and functional connections[12,44,45]; seed-based connectivity analyses have revealed correlations between CBF and rsFC in several brain regions[46,47]; and ICA has shown correlations between CBF and connectivity in several resting brain networks.[48]

In a prior study, the across-voxel CBF-FCS correlation and CBF/FCS ratio were used to characterize the coupling between the vascular response and neuronal activity in the brain.[12] For an individual, the CBF-FCS correlation across voxels reflects the consistency of spatial distribution between CBF and FCS at the whole gray matter level. The CBF/FCS ratio measures the amount of blood supply per unit of connectivity strength, which reflects the neurovascular coupling for a specific voxel or region. The across-voxel CBF-FCS correlation and CBF/FCS ratio could be used to identify changes in the neurovascular coupling in schizophrenia that cannot be detected by investigating the CBF and FCS separately.

Because brain regions with CBF and FCS changes in schizophrenia are spatially inconsistent (supplementary tables S1 and S2), we hypothesized that schizophrenia patients would show a reduced CBF-FCS coupling relative to healthy subjects. Because brain regions show different effect sizes and directions in CBF and FCS changes in schizophrenia, we hypothesized that schizophrenia patients would show region-specific changes in the CBF/FCS ratio. Brain regions with increased CBF and decreased FCS would show an increased CBF/FCS ratio in schizophrenia; in contrast, brain regions with decreased CBF and increased FCS would show a decreased CBF/FCS ratio. To test these hypotheses, we collected resting-state BOLD and ASL data from 89 schizophrenia patients and 90 sex- and age-matched healthy controls. The CBF-FCS coupling in a whole gray matter manner and CBF/FCS ratio in a voxel-wise manner were compared between the 2 groups.

Methods

Participants

A total of 179 right-handed individuals were recruited for this study, including 89 patients with schizophrenia and 90 healthy controls. Written informed consent was obtained from all participants, and the study was approved by the Ethics Committee of Tianjin Medical University General Hospital. Each patient met criteria for schizophrenia based on the Structured Clinical Interview for the DSM-IV Axis I Disorder (SCID, patient edition). The Positive and Negative Symptom Scale (PANSS)[49] was used to assess the severity of psychotic symptoms. All healthy controls were screened using the non-patient edition of the SCID to confirm an absence of psychiatric illnesses. The exclusion criteria for all participants were the following: MRI contraindications, the presence of a systemic medical illness or a central nervous system disorder that would affect brain function, a history of head trauma, a history of substance abuse within the past 3 months or a lifetime history of substance dependence. Additional exclusion criteria for the healthy controls included a history of psychiatric disease and first-degree relatives with a history of psychotic episodes. The detailed demographic and clinical data for these participants are shown in table 1.

Data Acquisition

MRI data were acquired using a 3.0-Tesla MR system (Discovery MR750, General Electric). Sagittal 3D T1-weighted images were acquired using a brain volume sequence with the following parameters: repetition time (TR) = 8.2 ms; echo time (TE) = 3.2 ms; inversion time (TI) = 450 ms; flip angle (FA) = 12°; field of view (FOV) = 256 mm × 256 mm; matrix = 256 × 256; slice thickness = 1 mm, no gap; 188 sagittal slices; and acquisition

Table 1. Demographic and Clinical Characteristics of the Schizophrenia Patients and Healthy Controls

Characteristics	Schizophrenia Patients	Healthy Controls	Statistics	*P* Value
Number of subjects	89	90		
Age (y)	33.5 ± 7.8	33.3 ± 10.2	$t = 0.118$	.906
Sex (female/male)	40/49	48/42	$\chi^2 = 1.260$	.262
FD	0.113 ± 0.056	0.114 ± 0.061	$t = 0.102$	.919
Antipsychotic dosage (mg/d) (chlorpromazine equivalents)	458.9 ± 343.3	—		
Duration of illness (mo)	117.7 ± 90.7	—		
PANSS				
Positive score	17.0 ± 7.9	—		
Negative score	20.1 ± 8.8	—		
General score	34.0 ± 11.0	—		
Total score	71.1 ± 23.6	—		

Note: FD, frame-wise displacement; PANSS, The Positive and Negative Syndrome Scale. The data are shown as the mean ± SD.

time = 250 s. The resting-state perfusion imaging was performed using a pseudo-continuous ASL (pcASL) sequence with a 3D fast spin-echo acquisition and background suppression (TR/TE = 4886/10.5 ms; post-label delay = 2025 ms; spiral in readout of 8 arms with 512 sample points; FA = 111°; FOV = 240 mm × 240 mm; reconstruction matrix = 128 × 128; slice thickness = 4 mm, no gap; 40 axial slices; number of excitation = 3; and acquisition time = 284 s). The label and control whole-brain image volumes required 8 TRs, respectively. A total of 3 pairs of label and control volumes were acquired. Resting-state BOLD images were acquired using a gradient-echo single-shot echo planar imaging (GRE-SS-EPI) sequence with the following parameters: TR/TE = 2000/45 ms; FOV = 220 mm × 220 mm; matrix = 64 × 64; FA = 90°; slice thickness = 4 mm; gap = 0.5 mm; 32 interleaved transverse slices; 180 volumes; and acquisition time = 370 s. All subjects were instructed to keep their eyes closed, relax, move as little as possible, think of nothing in particular, and stay awake during the scans.

CBF Analysis

An ASL difference image was calculated using a single-compartment model[50] after subtracting the label image from the control image. The 3 ASL difference images were averaged to calculate the CBF maps in combination with the proton-density-weighted reference images.[51] SPM8 software was used to normalize the CBF images to the Montreal Neurological Institute (MNI) space using the following steps: (1) the native ASL difference images of the healthy controls were non-linearly normalized to the MNI space and then averaged to generate a study-specific standard ASL template; (2) the native ASL difference image of each subject was non-linearly co-registered to the study-specific standard ASL template; and (3) the CBF image of each subject was written into the MNI space using the deformation parameter derived from the prior step and was resliced into a 3-mm cubic voxel. Then, each co-registered CBF map was removed of non-brain tissue and spatially smoothed with a Gaussian kernel of 6 mm × 6 mm × 6 mm full-width at half maximum (FWHM).

fMRI Data Preprocessing

The detailed preprocessing steps of the BOLD data are described in the supplementary materials.

Whole Gray Matter Functional Connectivity Analysis

We computed Pearson's correlation coefficients between the BOLD time courses of all pairs of voxels within the gray matter mask (N_{voxels} = 34 911) and obtained a whole gray matter functional connectivity matrix for each participant. Because removal of the global signal may induce controversial negative correlations,[52,53] we restricted our analysis to positive correlations above a threshold of 0.2 to eliminate weak correlations possibly arising from background noise.[13,14,17,54] This correlation threshold was selected because lower thresholds may include false-positive connectivity and higher thresholds may exclude some meaningful connectivity. The entry was zero if a functional connectivity was smaller than the threshold. For a given voxel x_0, the FCS was computed as the average of functional connectivity between x_0 and all other voxels including entries of zero. The FCS maps were spatially smoothed with a 6 mm × 6 mm × 6 mm FWHM Gaussian kernel.

Whole Gray Matter CBF-FCS Coupling Analysis

For each participant, both CBF and FCS maps were further normalized into *z*-scores by subtracting the mean and dividing by the SD of global values within the gray matter mask, so that they could be averaged and compared across subjects. To quantitatively evaluate the coupling between CBF and FCS, correlation analyses across voxels were performed for each participant. Because the neighboring voxels would be highly dependent on each other due to spatial preprocessing including registration and spatial smoothing, the effective degree of freedom df_{eff} in across-voxel correlation analyses would be much

smaller than the number of voxels within the gray matter mask. Therefore, the df_{eff} of across-voxel correlations was estimated using the following equation:

$$df_{eff} = \frac{N}{(FWHMx \times FWHMy \times FWHMz)/v} - 2$$

where v is the volume of a voxel ($3 \times 3 \times 3$ mm^3) and N is the number of voxels ($N = 34\,911$) used in the analyses. FWHMx × FWHMy × FWHMz were the average smoothness of the CBF and FCS maps ($14.0 \times 15.5 \times 20.1$ mm^3) estimated using the software REST[55] (http://www.restfmri.net/). The df_{eff} of across-voxel correlations in this study was 214. Accordingly, each participant had a CBF-FCS correlation coefficient value that reflected the consistency of spatial distribution between CBF and FCS at the whole gray matter level.[12] A 2-sample t test was then used to compare the difference in CBF-FCS correlation coefficients between schizophrenia patients and healthy controls.

CBF/FCS Ratio Analysis

To evaluate the amount of blood supply per unit of connectivity strength, we computed the CBF/FCS ratio (both were original values without z-transformation) of each voxel. To increase normality, the CBF/FCS ratio of each voxel for each participant was transformed into a z-score. The intergroup differences in CBF/FCS ratio were tested in a voxel-wise manner using a 2-sample t test with age and sex as the nuisance variables. Multiple comparisons were corrected using a voxel-wise false discovery rate (FDR) method with a corrected threshold of $P < .05$. For each participant, the mean CBF/FCS ratio of each cluster with significant group differences was extracted and used for region of interest (ROI)-based analyses. A non-parametric Spearman's rank correlation analysis was performed to test the association between the CBF/FCS ratio of each significant ROI and the severity of psychotic symptoms (positive, negative, and general scores of the PANSS). Multiple comparisons were corrected using the Bonferroni method ($P < .05/45 = .0011$).

Voxel-Wise Comparisons in CBF and FCS

To better understand what may drive the differences in CBF/FCS ratio, we compared the CBF and FCS differences between the 2 groups in a voxel-wise manner while controlling for age and sex. Multiple comparisons were also corrected using a voxel-wise FDR method ($P < .05$). The intergroup difference maps of the CBF, FCS, and CBF/FCS ratio were projected onto an overlay map to show what drove the differences in CBF/FCS ratio.

Effects of Antipsychotic Medications

Prior studies have revealed effects of antipsychotic medications on resting-state CBF.[56,57] To test the possible effects of antipsychotic medications on CBF-related analyses, we performed correlation analyses between antipsychotic dosages of chlorpromazine equivalents and imaging measurements (including global CBF of the whole gray matter, and voxel-wise CBF and CBF/FCS ratio with significant intergroup differences in the respective measures) in schizophrenia patients ($P < .05$, uncorrected).

Validation Analysis

In the FCS computation, we used a correlation coefficient threshold of 0.2 to eliminate weak correlations possibly arising from noise signals. To further evaluate the reproducibility of our main results, we re-calculated the FCS maps using 2 other correlation thresholds (ie, 0.1 and 0.3) and then repeated all of the analyses. Given that schizophrenia patients have shown gray matter atrophy,[58,59] we repeated the voxel-wise CBF/FCS ratio comparisons with the gray matter volume (GMV) of each voxel as an additional covariate of no interest to exclude the effect of gray matter atrophy. Prior studies have reported significant effects of age and sex on resting-state CBF[60,61] and FCS[62,63] in healthy subjects, so we tested the effects of age (correlation analysis) and sex (comparison between females and males) on the global CBF and FCS of the whole gray matter in controls and patients, respectively. We also repeated the voxel-wise comparisons for CBF, FCS, and CBF/FCS ratio without controlling for the effects of age and sex.

Results

Spatial Distribution of the FCS, CBF and CBF/FCS Ratio

Schizophrenia patients and healthy controls exhibited similar spatial distributions of FCS, CBF and CBF/FCS ratio (figure 1). Brain regions with higher CBF were mostly located in the posterior cingulate cortex/precuneus, medial prefrontal cortex, anterior cingulate cortex, lateral temporal and parietal cortices that comprise the default mode network (DMN), and in the insula, lateral prefrontal cortex, sensorimotor and visual cortices. Brain regions with higher FCS were primarily distributed in the DMN, lateral prefrontal cortex, and visual cortex. The CBF/FCS ratio was greater in the medial prefrontal cortex, anterior cingulate cortex, sensorimotor cortex, and thalamus.

Whole Gray Matter CBF-FCS Coupling Changes in Schizophrenia

Compared with healthy controls, schizophrenia patients exhibited a decreased global CBF (patients: 51.5 ± 9.3 ml/100g/min; controls: 55.5 ± 8.8 ml/100g/min; 2-sample t test, $t = -3.0$, $P = .003$) and global FCS (patients: 0.0378 ± 0.0058; controls: 0.0393 ± 0.0042; 2-sample t test, $t = -2.1$, $P = .038$) in the whole gray matter. Although CBF was significantly correlated with FCS in both schizophrenia

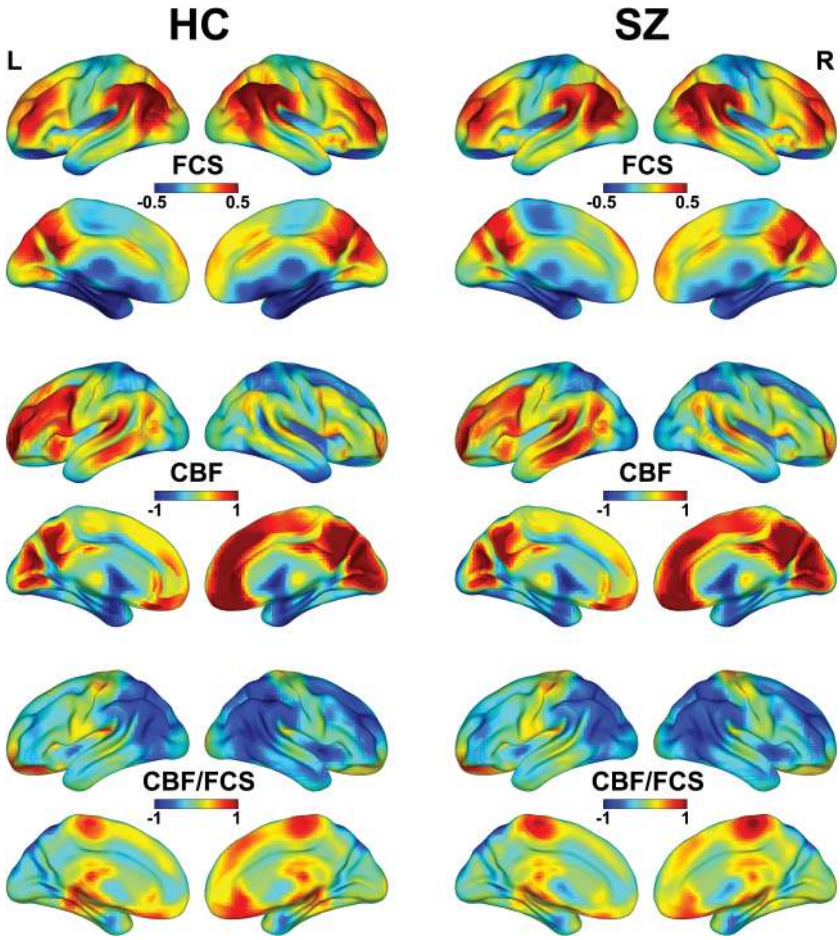

Fig. 1. Spatial distribution maps of FCS, CBF, and CBF/FCS ratio. The FCS, CBF, and CBF/FCS ratio maps are normalized to *z*-scores and averaged across subjects within groups. The FCS is calculated using a connectivity threshold of 0.2. CBF, cerebral blood flow; FCS, functional connectivity strength; HC, healthy controls; L, left; R, right; SZ, schizophrenia patients.

and control groups (figure 2A), schizophrenia patients had a significantly reduced CBF-FCS coupling ($t = -2.5$, $P = .015$, 15% reduction) relative to healthy controls (figure 2B).

CBF-FCS Ratio Changes in Schizophrenia

Compared with healthy controls, schizophrenia patients exhibited decreased CBF/FCS ratio in the hippocampus and thalamus bilaterally, and the left middle frontal gyrus, insula and supplementary motor area as well as increased CBF/FCS ratio in the sensorimotor cortex, putamen and mid-cingulate cortex bilaterally, the left angular gyrus and fusiform gyrus, and the right lingual gyrus ($P < .05$, FDR corrected) (figure 3 and supplementary table S3).

Correlation Between CBF/FCS Ratio and Psychotic Symptoms

The correlations between the CBF/FCS ratio of each significant ROI and the severity of psychotic symptoms (the positive, negative, and general scores of the PANSS) are shown in supplementary table S4. In schizophrenia patients, we only found a trend towards a significant correlation between the CBF/FCS ratio in the left hippocampus and the PANSS negative score (Spearman's $\rho = -0.231$, $P = .029$). However, the significance did not remain after Bonferroni correction ($P < .05/45 = .0011$).

CBF and FCS Changes in Schizophrenia

Compared with healthy controls, schizophrenia patients showed decreased CBF bilaterally in the prefrontal cortex, anterior cingulate cortex, occipital cortex, insula and supplementary motor area as well as increased CBF bilaterally in the temporal cortex, sensorimotor cortex, mid-cingulate cortex, striatum and thalamus ($P < .05$, FDR corrected) (supplementary figures S1 and S2). Schizophrenia patients exhibited decreased FCS in the bilateral occipital cortex, the left inferior parietal lobule and the right sensorimotor cortex as well as increased FCS in the bilateral temporal cortex, hippocampus, striatum and thalamus, and the left prefrontal cortex ($P < .05$, FDR corrected) (supplementary figures S3 and S4).

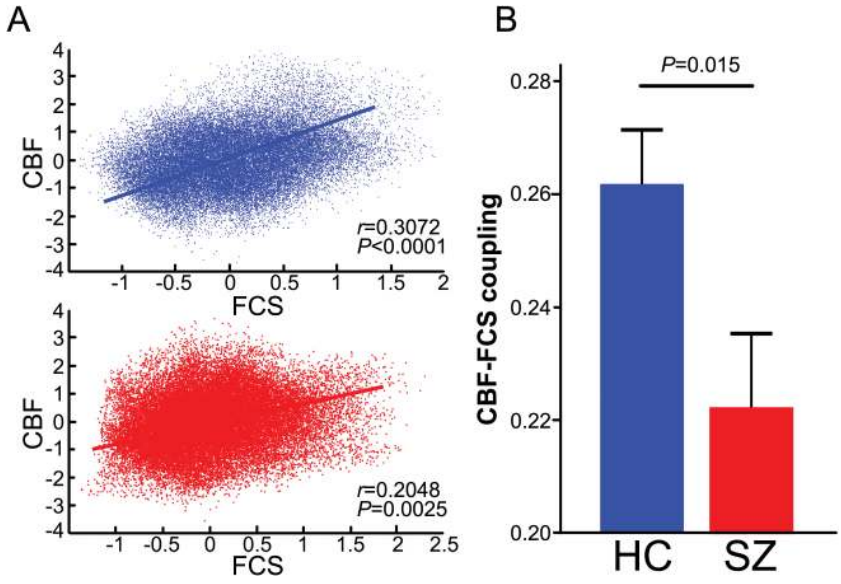

Fig. 2. Whole gray matter level CBF-FCS coupling changes in schizophrenia. Scatter plots (A) of the spatial correlations across voxels between CBF and FCS in a healthy subject (blue) and a schizophrenia patient (red), respectively. The mean whole gray matter level CBF-FCS coupling in schizophrenia patients and healthy controls (B). Although CBF is significantly correlated with FCS in both schizophrenia and control groups, schizophrenia patients have a significantly reduced CBF-FCS coupling relative to healthy controls. Significant difference was found between patients and controls on CBF-FCS correlation coefficients across voxels. Error bars represent the SE. CBF, cerebral blood flow; FCS, functional connectivity strength; HC, healthy controls; SZ, schizophrenia patients.

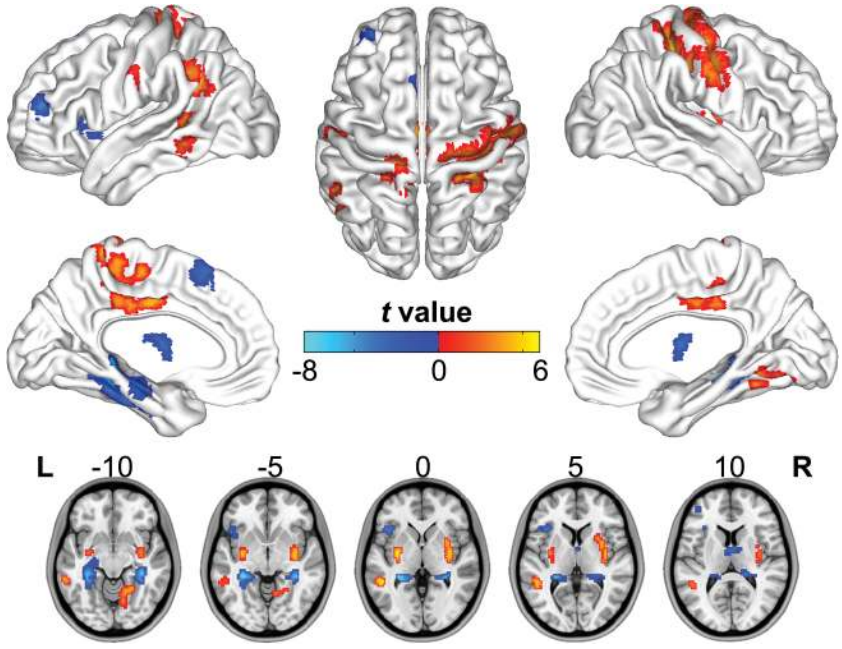

Fig. 3. Group differences in CBF/FCS ratio between schizophrenia patients and healthy controls ($P < .05$, FDR corrected) while controlling for the effects of age and sex. The warm and cold colors denote significantly increased and decreased CBF/FCS ratio in the schizophrenia patients, respectively. CBF, cerebral blood flow; FCS, functional connectivity strength; L, left; R, right.

Associations Between the CBF/FCS Ratio and CBF and FCS Changes in Patients

The relationships between the CBF/FCS ratio (red) and CBF (blue) and FCS (green) changes in schizophrenia patients are shown in supplementary figure S5. The red-colored regions were those with a CBF/FCS ratio but without CBF and FCS changes, including parts of the left paracentral lobule, sensorimotor cortex and superior marginal gyrus, and the right lingual gyrus. The overlap (pink) between the CBF/FCS ratio and CBF changes was mainly located in the bilateral mid-cingulate cortex and putamen, the left middle frontal gyrus, insula, supplementary motor

area and fusiform gyrus. The overlap (yellow) between the CBF/FCS ratio and FCS changes was primarily distributed in the bilateral hippocampus, anterior thalamus, and the right sensorimotor cortex. Parts of the bilateral hippocampus and the right sensorimotor cortex (white) exhibited significant changes in all 3 measurements.

Effects of Antipsychotic Medications on CBF-Related Measures

We did not find a significant correlation (Spearman's $\rho = -0.205$, $P = .053$) between antipsychotic dosages and global CBF of the whole gray matter. Antipsychotic dosages were positively correlated with the CBF in the bilateral striatum and temporal cortex, the left paracentral lobule and middle cingulate cortex as well as negatively correlated with the CBF in the bilateral occipital and lateral prefrontal cortex, and the left parietal cortex ($P < .05$, uncorrected) (supplementary figure S6). However, these correlations were not significant after FDR correction for multiple comparisons. Moreover, we did not find any significant correlations between antipsychotic dosages and the CBF/FCS ratio ($P < .05$, uncorrected).

Validation Analyses

In the FCS calculation, we used an arbitrary correlation threshold of $r = .2$. To test the potential effect of the correlation thresholds on our results, we repeated our analyses using correlation thresholds of .1 and .3. The spatial distributions of FCS and CBF/FCS ratio at $r = .1$ (supplementary figure S7) and $r = .3$ (supplementary figure S8) were very similar to those at $r = .2$. Compared with healthy controls, schizophrenia patients still had significantly reduced whole gray matter CBF-FCS coupling at $r = .1$ ($t = -2.2$, $P = .029$, 14% reduction) (supplementary figure S9) and $r = .3$ ($t = -2.6$, $P = .010$, 16% reduction) (supplementary figure S10). Furthermore, the brain regions showing significant intergroup differences in CBF/FCS ratio at $r = .2$ were largely preserved at $r = .1$ (supplementary figure S11) and $r = .3$ (supplementary figure S12). Finally, the brain regions with significant FCS differences at $r = .1$ (supplementary figure S13) and $r = .3$ (supplementary figure S14) were consistent with those at $r = .2$.

Because GMV atrophy may affect CBF/FCS ratio changes in schizophrenia, we also repeated intergroup comparisons in the CBF/FCS ratio while controlling for the GMV. We found that the spatial distribution of brain regions with altered CBF/FCS ratio after GMV correction was similar to that without GMV correction (supplementary figure S15), suggesting that most of the CBF/FCS ratio alterations were independent of GMV atrophy in schizophrenia.

We found that both age and sex significantly affected global CBF of the whole gray matter in the healthy controls, ie, age was negatively correlated with the mean CBF ($r = -.227$, $P = .032$) and females had greater mean CBF than males ($t = 2.807$, $P = .006$). We did not find any significant age or sex effects on the mean FCS ($r = .098$, $P = .358$; $t = -0.298$, $P = .767$) in healthy controls, or any significant age or sex effects on the whole gray matter mean CBF ($r = -.093$, $P = .385$; $t = 1.537$, $P = .128$) and FCS ($r = -.051$, $P = .638$; $t = 0.956$, $P = .342$) in schizophrenia patients. In addition, we found similar spatial distribution of brain regions exhibiting significant intergroup differences in CBF, FCS and CBF/FCS ratio with and without controlling for the effects of age and sex (supplementary figures S16–18).

Discussion

To our knowledge, this is the first study to investigate CBF-FCS coupling changes in schizophrenia by combining BOLD and ASL techniques. Whole gray matter CBF-FCS coupling was reduced in schizophrenia patients relative to healthy controls. Moreover, schizophrenia patients showed decreased CBF/FCS ratio in cognitive- and emotional-related regions and increased CBF/FCS ratio in sensorimotor regions. These findings may improve our understanding of the neural mechanisms of schizophrenia from the perspective of neurovascular coupling.

We found CBF changes in schizophrenia, which may be explained by the following mechanisms. First, CBF changes may reflect altered neuronal activity in schizophrenia, because CBF changes are governed by neuronal activity based on the neurovascular coupling hypothesis.[41] For example, a brain region with enhanced neuronal activity has higher metabolic demand, resulting in increased perfusion.[42] Second, CBF changes may be the result of changes in neurotransmitters (eg, dopamine[64,65] and GABA[66,67]) and non-specific agents (eg, nitric oxide[68,69]) in schizophrenia, because these chemicals also play a role in modulating vascular response.[70–72] Finally, CBF changes may be related to microvasculature alterations associated with neuroinflammation in schizophrenia,[73–75] resulting in imprecise regulation of CBF.[76]

FCS depicts a whole-brain functional connectivity profile of each voxel from a global network perspective,[12–15] and reflects the role of each voxel in information transmission in the whole brain network. The decreased FCS in schizophrenia may be the result of structural damage, ie, gray matter reduction[77,78] and white matter alterations.[2,79–81] The loss of structural integrity may impair the precise coordination of inter-regional functional synchronization.[82,83] In addition, schizophrenia patients also exhibit functional connectivity increase in certain neural systems,[84–86] consistent with findings in this study. Although antipsychotic treatment,[87] head motion,[88] and global signal correction[89,90] may be contributing factors, Fornito and Bullmore[3] provide the other possible mechanisms for

functional connectivity increase in schizophrenia: (1) a compensatory response to structural impairments; (2) an undifferentiated state of neural activity characterized by a breakdown of normally segregated neural activity; and (3) a paradoxical but topologically predictable effect of neurodevelopmentally driven reductions of the anatomical connections of network hubs.

Consistent with a previous study,[12] we found a significant across-voxel correlation between CBF and FCS in healthy subjects, representing a normal neurovascular coupling. The neurovascular coupling depends on the integrity of neurovascular unit (ie, neurons, glial cells, and vascular components).[91] In the unit, astrocytes play an important role in bridging neuronal activity and vascular response.[92,93] Although we also found across-voxel correlation between CBF and FCS in schizophrenia patients, it was lower than healthy subjects, possibly indicating neurovascular decoupling in schizophrenia. One possible explanation for this neurovascular decoupling is the abnormal astrocytes in schizophrenia[94] that may reduce the connection between neuronal activity and the vascular response. Abnormal GABA interneurons in schizophrenia[66,67] may also contribute to neurovascular decoupling since normal GABA interneurons play an important role in modulating neurovascular coupling.[71,95] Additionally, other factors (eg, nitric oxide[68,69] and neuroinflammation[73–76]) that affect vascular components (CBF) but not neuronal activity (FCS), could also result in neurovascular decoupling.

In voxel-wise analyses, several brain regions without significant intergroup differences in CBF and FCS showed significant differences in CBF/FCS ratio between patients and controls. Further ROI-based analyses demonstrated that these regions showed relatively higher CBF and lower FCS in schizophrenia patients than those in healthy controls (supplementary figure S19). In this situation, the CBF/FCS ratio may enlarge the intergroup difference to identify abnormal regions in schizophrenia that cannot be found by the CBF or FCS analyses using the same statistical threshold. In contrast, in several regions with significant intergroup differences in CBF, FCS or both, the CBF/FCS ratio did not show significant differences between the 2 groups. Taken together, these findings indicate that the CBF, FCS and CBF/FCS ratio could provide complementary information and should be jointly used to reveal pathological changes in schizophrenia.

Schizophrenia patients showed decreased CBF/FCS ratio in the dorsolateral prefrontal cortex, insula, hippocampus and thalamus, which are mainly involved in cognitive control and emotional modulation.[96–100] Among them, the dorsolateral prefrontal cortex and insula showed reduced CBF and normal FCS, suggesting that the CBF/FCS ratio decrease in these regions is predominantly driven by the CBF decrease. The abnormality may at least partly account for the cognitive and behavioral deficits ascribed to these regions in schizophrenia.[101–103] In contrast, the hippocampus and thalamus exhibited normal CBF and increased FCS, indicating that the CBF/FCS ratio reduction in these regions is mainly driven by the FCS increase; this finding is consistent with previous studies reporting increased functional connectivity of the hippocampus[104] and thalamus[105,106] in schizophrenia. The thalamus is a crucial node of multiple functional circuits supporting cognitive functions, including memory and executive functions of attention and information processing.[100] The decreased CBF/FCS ratio in the thalamus may affect the thalamo-cortical circuits,[107,108] which may relate to cognitive impairments in schizophrenia.[109]

Patients with schizophrenia exhibited increased CBF/FCS ratio in the putamen, middle cingulate cortex, fusiform gyrus, sensorimotor cortex and lingual gyrus, which are mainly implicated in sensory processing and motor regulation. Impairments of these brain regions in schizophrenia have been extensively reported.[18,110–117] A number of studies have reported sensory and motor symptoms in schizophrenia, including somatosensory, auditory and visual dysfunctions[118,119] as well as abnormal involuntary movements, parkinsonism, neurological soft signs, catatonia, and psychomotor slowing.[120] The increased CBF/FCS ratio in the putamen, middle cingulate cortex and fusiform gyrus is predominantly driven by the increased CBF. Because we also found effects of antipsychotics on CBF in these regions, the increased CBF may be explained by the medication-induced dopamine turnover increase (antipsychotics—antagonizing D2 receptors—increased dopamine turnover—CBF increase).[56] In addition, the increased CBF/FCS ratio in the sensorimotor cortex is mainly driven by the decreased FCS, which has been consistently reported in schizophrenia.[17–19]

Our finding of a trend negative correlation between the CBF/FCS ratio in the hippocampus and the severity of negative symptoms indicates that more reduced CBF/FCS ratio (mainly driven by the FCS increase) is associated with more severe negative symptoms in schizophrenia. Previous studies have demonstrated that cognitive impairments correlate with negative symptoms more strongly than positive symptoms.[121] Structural imaging studies have shown that hippocampal volume is reduced in schizophrenia and is correlated with cognitive abilities and negative symptoms.[122,123] In a recent functional imaging study, resting-state hippocampal hyperactivity was found to be negatively correlated with cognition and positively correlated with negative symptoms in schizophrenia patients.[104] Given these findings, it is possible to speculate that intrinsic hyperactivity in the hippocampus reduces the region's ability to be recruited according to task demands, which contributes to impaired cognitive performance and negative symptoms.[104] Another possibility is that the reduced CBF/FCS ratio reflects neurovascular decoupling, which impairs the function of the hippocampus, possibly contributing to negative symptoms.

There are several limitations that should be mentioned in the present study. First, most of these schizophrenia

patients were receiving antipsychotic drug treatment, which could have influenced our interpretations. Future studies with medication-naïve, first-episode schizophrenia patients are required to eliminate medication effects and confirm the findings of this study. Second, CBF is an indirect measure of vascular response and FCS is an indirect measure of neuronal activity, which prevents us from drawing exact conclusions about the biological implications of these measurements. Third, the advantage of including zero entries is reflecting the mean FCS of each voxel; the disadvantage of including zero entries is including weak or meaningless connectivity in FCS calculation. The advantage of excluding zero entries is excluding weak or meaningless connectivity from FCS calculation; the disadvantage of excluding zero entries is exaggerating the contribution of strong connectivity to FCS. The choice is mainly dependent on the focus of research. In this study, we aimed to use the mean FCS of each voxel as a measure of neuronal activity. Thus, including zero entries is more appropriate. Finally, although we found a trend towards a significant correlation between the CBF/FCS ratio and the PANSS score, more sensitive and specific neuropsychological scales may provide further information on the functional significance of these CBF/FCS abnormalities.

In conclusion, we revealed a disrupted coupling between resting-state CBF and functional connectivity in schizophrenia by using a combination of BOLD and ASL techniques. Specifically, we found a decreased CBF/FCS ratio in higher-order brain systems involved in cognitive control and emotional modulation, and an increased CBF/FCS ratio in lower-order brain systems implicated in sensory processing and motor regulation. These findings suggest that the neurovascular decoupling in the brain may be a potential neural mechanism involved in the pathophysiology of schizophrenia.

Supplementary Material

Supplementary data are available at *Schizophrenia Bulletin* online.

Funding

Natural Science Foundation of China (81425013, 81501451, 91332113 and 81271551); Tianjin Key Technology R&D Program (14ZCZDSY00018).

Acknowledgments

The authors declare no conflict of interest.

References

1. Lewis DA, Lieberman JA. Catching up on schizophrenia: natural history and neurobiology. *Neuron*. 2000;28:325–334.
2. Fitzsimmons J, Kubicki M, Shenton ME. Review of functional and anatomical brain connectivity findings in schizophrenia. *Curr Opin Psychiatry*. 2013;26:172–187.
3. Fornito A, Bullmore ET. Reconciling abnormalities of brain network structure and function in schizophrenia. *Curr Opin Neurobiol*. 2015;30:44–50.
4. van den Heuvel MP, Fornito A. Brain networks in schizophrenia. *Neuropsychol Rev*. 2014;24:32–48.
5. Biswal B, Yetkin FZ, Haughton VM, Hyde JS. Functional connectivity in the motor cortex of resting human brain using echo-planar MRI. *Magn Reson Med*. 1995;34:537–541.
6. Fox MD, Raichle ME. Spontaneous fluctuations in brain activity observed with functional magnetic resonance imaging. *Nat Rev Neurosci*. 2007;8:700–711.
7. Yu Q, Allen EA, Sui J, Arbabshirani MR, Pearlson G, Calhoun VD. Brain connectivity networks in schizophrenia underlying resting state functional magnetic resonance imaging. *Curr Top Med Chem*. 2012;12:2415–2425.
8. Karbasforoushan H, Woodward ND. Resting-state networks in schizophrenia. *Curr Top Med Chem*. 2012;12:2404–2414.
9. Nair A, Keown CL, Datko M, Shih P, Keehn B, Müller RA. Impact of methodological variables on functional connectivity findings in autism spectrum disorders. *Hum Brain Mapp*. 2014;35:4035–4048.
10. Damoiseaux JS, Rombouts SA, Barkhof F, et al. Consistent resting-state networks across healthy subjects. *Proc Natl Acad Sci U S A*. 2006;103:13848–13853.
11. van de Ven VG, Formisano E, Prvulovic D, Roeder CH, Linden DE. Functional connectivity as revealed by spatial independent component analysis of fMRI measurements during rest. *Hum Brain Mapp*. 2004;22:165–178.
12. Liang X, Zou Q, He Y, Yang Y. Coupling of functional connectivity and regional cerebral blood flow reveals a physiological basis for network hubs of the human brain. *Proc Natl Acad Sci U S A*. 2013;110:1929–1934.
13. Wang L, Dai Z, Peng H, et al. Overlapping and segregated resting-state functional connectivity in patients with major depressive disorder with and without childhood neglect. *Hum Brain Mapp*. 2014;35:1154–1166.
14. Wang L, Xia M, Li K, et al. The effects of antidepressant treatment on resting-state functional brain networks in patients with major depressive disorder. *Hum Brain Mapp*. 2015;36:768–778.
15. Buckner RL, Sepulcre J, Talukdar T, et al. Cortical hubs revealed by intrinsic functional connectivity: mapping, assessment of stability, and relation to Alzheimer's disease. *J Neurosci*. 2009;29:1860–1873.
16. Guo W, Liu F, Xiao C, et al. Increased short-range and long-range functional connectivity in first-episode, medication-naive schizophrenia at rest. *Schizophr Res*. 2015;166:144–150.
17. Wang X, Xia M, Lai Y, et al. Disrupted resting-state functional connectivity in minimally treated chronic schizophrenia. *Schizophr Res*. 2014;156:150–156.
18. Chen X, Duan M, Xie Q, et al. Functional disconnection between the visual cortex and the sensorimotor cortex suggests a potential mechanism for self-disorder in schizophrenia. *Schizophr Res*. 2015;166:151–157.
19. Tomasi D, Volkow ND. Mapping small-world properties through development in the human brain: disruption in schizophrenia. *PLoS One*. 2014;9:e96176.
20. Raichle ME, MacLeod AM, Snyder AZ, Powers WJ, Gusnard DA, Shulman GL. A default mode of brain function. *Proc Natl Acad Sci U S A*. 2001;98:676–682.

21. Vaishnavi SN, Vlassenko AG, Rundle MM, Snyder AZ, Mintun MA, Raichle ME. Regional aerobic glycolysis in the human brain. *Proc Natl Acad Sci U S A*. 2010;107:17757–17762.
22. Andreasen NC, O'Leary DS, Flaum M, et al. Hypofrontality in schizophrenia: distributed dysfunctional circuits in neuroleptic-naïve patients. *Lancet*. 1997;349:1730–1734.
23. Catafau AM, Parellada E, Lomeña FJ, et al. Prefrontal and temporal blood flow in schizophrenia: resting and activation technetium-99m-HMPAO SPECT patterns in young neuroleptic-naive patients with acute disease. *J Nucl Med*. 1994;35:935–941.
24. Kanahara N, Sekine Y, Haraguchi T, et al. Orbitofrontal cortex abnormality and deficit schizophrenia. *Schizophr Res*. 2013;143:246–252.
25. Kanahara N, Shimizu E, Sekine Y, et al. Does hypofrontality expand to global brain area in progression of schizophrenia?: a cross-sectional study between first-episode and chronic schizophrenia. *Prog Neuropsychopharmacol Biol Psychiatry*. 2009;33:410–415.
26. Kawasaki Y, Maeda Y, Suzuki M, et al. SPECT analysis of regional cerebral blood flow changes in patients with schizophrenia during the Wisconsin Card Sorting Test. *Schizophr Res*. 1993;10:109–116.
27. Malaspina D, Harkavy-Friedman J, Corcoran C, et al. Resting neural activity distinguishes subgroups of schizophrenia patients. *Biol Psychiatry*. 2004;56:931–937.
28. Mathew RJ, Wilson WH, Tant SR, Robinson L, Prakash R. Abnormal resting regional cerebral blood flow patterns and their correlates in schizophrenia. *Arch Gen Psychiatry*. 1988;45:542–549.
29. Rubin P, Holm S, Madsen PL, et al. Regional cerebral blood flow distribution in newly diagnosed schizophrenia and schizophreniform disorder. *Psychiatry Res*. 1994;53:57–75.
30. Weinberger DR, Berman KF, Zec RF. Physiologic dysfunction of dorsolateral prefrontal cortex in schizophrenia. I. Regional cerebral blood flow evidence. *Arch Gen Psychiatry*. 1986;43:114–124.
31. Golay X, Hendrikse J, Lim TC. Perfusion imaging using arterial spin labeling. *Top Magn Reson Imaging*. 2004;15:10–27.
32. Williams DS, Detre JA, Leigh JS, Koretsky AP. Magnetic resonance imaging of perfusion using spin inversion of arterial water. *Proc Natl Acad Sci U S A*. 1992;89:212–216.
33. Kindler J, Jann K, Homan P, et al. Static and dynamic characteristics of cerebral blood flow during the resting state in schizophrenia. *Schizophr Bull*. 2015;41:163–170.
34. Liu J, Qiu M, Constable RT, Wexler BE. Does baseline cerebral blood flow affect task-related blood oxygenation level dependent response in schizophrenia? *Schizophr Res*. 2012;140:143–148.
35. Pinkham A, Loughead J, Ruparel K, et al. Resting quantitative cerebral blood flow in schizophrenia measured by pulsed arterial spin labeling perfusion MRI. *Psychiatry Res*. 2011;194:64–72.
36. Scheef L, Manka C, Daamen M, et al. Resting-state perfusion in nonmedicated schizophrenic patients: a continuous arterial spin-labeling 3.0-T MR study. *Radiology*. 2010;256:253–260.
37. Walther S, Federspiel A, Horn H, et al. Resting state cerebral blood flow and objective motor activity reveal basal ganglia dysfunction in schizophrenia. *Psychiatry Res*. 2011;192:117–124.
38. Bullmore E, Sporns O. The economy of brain network organization. *Nat Rev Neurosci*. 2012;13:336–349.
39. Raichle ME, Gusnard DA. Appraising the brain's energy budget. *Proc Natl Acad Sci U S A*. 2002;99:10237–10239.
40. Raichle ME, Mintun MA. Brain work and brain imaging. *Annu Rev Neurosci*. 2006;29:449–476.
41. Kuschinsky W. Coupling of function, metabolism, and blood flow in the brain. *Neurosurg Rev*. 1991;14:163–168.
42. Venkat P, Chopp M, Chen J. New insights into coupling and uncoupling of cerebral blood flow and metabolism in the brain. *Croat Med J*. 2016;57:223–228.
43. Tomasi D, Wang GJ, Volkow ND. Energetic cost of brain functional connectivity. *Proc Natl Acad Sci U S A*. 2013;110:13642–13647.
44. Liang X, Connelly A, Calamante F. Graph analysis of resting-state ASL perfusion MRI data: nonlinear correlations among CBF and network metrics. *Neuroimage*. 2014;87:265–275.
45. Várkuti B, Cavusoglu M, Kullik A, et al. Quantifying the link between anatomical connectivity, gray matter volume and regional cerebral blood flow: an integrative MRI study. *PLoS One*. 2011;6:e14801.
46. Li Z, Zhu Y, Childress AR, Detre JA, Wang Z. Relations between BOLD fMRI-derived resting brain activity and cerebral blood flow. *PLoS One*. 2012;7:e44556.
47. Zou Q, Wu CW, Stein EA, Zang Y, Yang Y. Static and dynamic characteristics of cerebral blood flow during the resting state. *Neuroimage*. 2009;48:515–524.
48. Jann K, Gee DG, Kilroy E, et al. Functional connectivity in BOLD and CBF data: similarity and reliability of resting brain networks. *Neuroimage*. 2015;106:111–122.
49. Kay SR, Fiszbein A, Opler LA. The positive and negative syndrome scale (PANSS) for schizophrenia. *Schizophr Bull*. 1987;13:261–276.
50. Buxton RB, Frank LR, Wong EC, Siewert B, Warach S, Edelman RR. A general kinetic model for quantitative perfusion imaging with arterial spin labeling. *Magn Reson Med*. 1998;40:383–396.
51. Xu G, Rowley HA, Wu G, et al. Reliability and precision of pseudo-continuous arterial spin labeling perfusion MRI on 3.0 T and comparison with 15O-water PET in elderly subjects at risk for Alzheimer's disease. *NMR Biomed*. 2010;23:286–293.
52. Fox MD, Zhang D, Snyder AZ, Raichle ME. The global signal and observed anticorrelated resting state brain networks. *J Neurophysiol*. 2009;101:3270–3283.
53. Murphy K, Birn RM, Handwerker DA, Jones TB, Bandettini PA. The impact of global signal regression on resting state correlations: are anti-correlated networks introduced? *Neuroimage*. 2009;44:893–905.
54. Liu F, Zhu C, Wang Y, et al. Disrupted cortical hubs in functional brain networks in social anxiety disorder. *Clin Neurophysiol*. 2015;126:1711–1716.
55. Song XW, Dong ZY, Long XY, et al. REST: a toolkit for resting-state functional magnetic resonance imaging data processing. *PLoS One*. 2011;6:e25031.
56. Goozée R, Handley R, Kempton MJ, Dazzan P. A systematic review and meta-analysis of the effects of antipsychotic medications on regional cerebral blood flow (rCBF) in schizophrenia: association with response to treatment. *Neurosci Biobehav Rev*. 2014;43:118–136.
57. Handley R, Zelaya FO, Reinders AA, et al. Acute effects of single-dose aripiprazole and haloperidol on resting cerebral blood flow (rCBF) in the human brain. *Hum Brain Mapp*. 2013;34:272–282.

58. Crow TJ, Frith CD, Johnstone EC, Owens DG. Schizophrenia and cerebral atrophy. *Lancet*. 1980;1:1129–1130.
59. Weinberger DR, Wyatt RJ. Schizophrenia and cerebral atrophy. *Lancet*. 1980;1:1130.
60. Pagani M, Salmaso D, Jonsson C, et al. Regional cerebral blood flow as assessed by principal component analysis and (99m)Tc-HMPAO SPET in healthy subjects at rest: normal distribution and effect of age and gender. *Eur J Nucl Med Mol Imaging*. 2002;29:67–75.
61. Parkes LM, Rashid W, Chard DT, Tofts PS. Normal cerebral perfusion measurements using arterial spin labeling: reproducibility, stability, and age and gender effects. *Magn Reson Med*. 2004;51:736–743.
62. Tomasi D, Volkow ND. Gender differences in brain functional connectivity density. *Hum Brain Mapp*. 2012;33:849–860.
63. Tomasi D, Volkow ND. Aging and functional brain networks. *Mol Psychiatry*. 2012;17:471, 549-458.
64. Abi-Dargham A. Schizophrenia: overview and dopamine dysfunction. *J Clin Psychiatry*. 2014;75:e31.
65. Maia TV, Frank MJ. An integrative perspective on the role of dopamine in schizophrenia. *Biol Psychiatry*. 2017;81:52–66.
66. Benes FM. The GABA system in schizophrenia: cells, molecules and microcircuitry. *Schizophr Res*. 2015;167:1–3.
67. Taylor SF, Tso IF. GABA abnormalities in schizophrenia: a methodological review of in vivo studies. *Schizophr Res*. 2015;167:84–90.
68. Bernstein HG, Keilhoff G, Steiner J, Dobrowolny H, Bogerts B. Nitric oxide and schizophrenia: present knowledge and emerging concepts of therapy. *CNS Neurol Disord Drug Targets*. 2011;10:792–807.
69. Pitsikas N. The role of nitric oxide synthase inhibitors in schizophrenia. *Curr Med Chem*. 2016;23:2692–2705.
70. Tayebati SK, Lokhandwala MF, Amenta F. Dopamine and vascular dynamics control: present status and future perspectives. *Curr Neurovasc Res*. 2011;8:246–257.
71. Cauli B, Tong XK, Rancillac A, et al. Cortical GABA interneurons in neurovascular coupling: relays for subcortical vasoactive pathways. *J Neurosci*. 2004;24:8940–8949.
72. Akgören N, Fabricius M, Lauritzen M. Importance of nitric oxide for local increases of blood flow in rat cerebellar cortex during electrical stimulation. *Proc Natl Acad Sci U S A*. 1994;91:5903–5907.
73. Kirkpatrick B, Miller BJ. Inflammation and schizophrenia. *Schizophr Bull*. 2013;39:1174–1179.
74. Trépanier MO, Hopperton KE, Mizrahi R, Mechawar N, Bazinet RP. Postmortem evidence of cerebral inflammation in schizophrenia: a systematic review. *Mol Psychiatry*. 2016;21:1009–1026.
75. Chaves C, Zuardi AW, Hallak JE. The role of inflammation in schizophrenia: an overview. *Trends Psychiatry Psychother*. 2015;37:104–105.
76. Hanson DR, Gottesman II. Theories of schizophrenia: a genetic-inflammatory-vascular synthesis. *BMC Med Genet*. 2005;6:7.
77. Haijma SV, Van Haren N, Cahn W, Koolschijn PC, Hulshoff Pol HE, Kahn RS. Brain volumes in schizophrenia: a meta-analysis in over 18 000 subjects. *Schizophr Bull*. 2013;39:1129–1138.
78. Vita A, De Peri L, Deste G, Sacchetti E. Progressive loss of cortical gray matter in schizophrenia: a meta-analysis and meta-regression of longitudinal MRI studies. *Transl Psychiatry*. 2012;2:e190.
79. Fornito A, Zalesky A, Pantelis C, Bullmore ET. Schizophrenia, neuroimaging and connectomics. *Neuroimage*. 2012;62:2296–2314.
80. Pettersson-Yeo W, Allen P, Benetti S, McGuire P, Mechelli A. Dysconnectivity in schizophrenia: where are we now? *Neurosci Biobehav Rev*. 2011;35:1110–1124.
81. Wheeler AL, Voineskos AN. A review of structural neuroimaging in schizophrenia: from connectivity to connectomics. *Front Hum Neurosci*. 2014;8:653.
82. Honey CJ, Kötter R, Breakspear M, Sporns O. Network structure of cerebral cortex shapes functional connectivity on multiple time scales. *Proc Natl Acad Sci U S A*. 2007;104:10240–10245.
83. Rubinov M, Sporns O, van Leeuwen C, Breakspear M. Symbiotic relationship between brain structure and dynamics. *BMC Neurosci*. 2009;10:55.
84. Fornito A, Harrison BJ, Goodby E, et al. Functional dysconnectivity of corticostriatal circuitry as a risk phenotype for psychosis. *JAMA Psychiatry*. 2013;70:1143–1151.
85. Whitfield-Gabrieli S, Thermenos HW, Milanovic S, et al. Hyperactivity and hyperconnectivity of the default network in schizophrenia and in first-degree relatives of persons with schizophrenia. *Proc Natl Acad Sci U S A*. 2009;106:1279–1284.
86. Hoffman RE, Fernandez T, Pittman B, Hampson M. Elevated functional connectivity along a corticostriatal loop and the mechanism of auditory/verbal hallucinations in patients with schizophrenia. *Biol Psychiatry*. 2011;69:407–414.
87. Nejad AB, Ebdrup BH, Glenthøj BY, Siebner HR. Brain connectivity studies in schizophrenia: unravelling the effects of antipsychotics. *Curr Neuropharmacol*. 2012;10:219–230.
88. Power JD, Barnes KA, Snyder AZ, Schlaggar BL, Petersen SE. Spurious but systematic correlations in functional connectivity MRI networks arise from subject motion. *Neuroimage*. 2012;59:2142–2154.
89. Saad ZS, Gotts SJ, Murphy K, et al. Trouble at rest: how correlation patterns and group differences become distorted after global signal regression. *Brain Connect*. 2012;2:25–32.
90. Yang GJ, Murray JD, Repovs G, et al. Altered global brain signal in schizophrenia. *Proc Natl Acad Sci U S A*. 2014;111:7438–7443.
91. Hawkins BT, Davis TP. The blood-brain barrier/neurovascular unit in health and disease. *Pharmacol Rev*. 2005;57:173–185.
92. Howarth C. The contribution of astrocytes to the regulation of cerebral blood flow. *Front Neurosci*. 2014;8:103.
93. Stobart JL, Anderson CM. Multifunctional role of astrocytes as gatekeepers of neuronal energy supply. *Front Cell Neurosci*. 2013;7:38.
94. Steffek AE. *The Role of Astrocytes in the Pathophysiology of Schizophrenia* [doctoral dissertation]. The University of Michigan; 2007.
95. Kocharyan A, Fernandes P, Tong XK, Vaucher E, Hamel E. Specific subtypes of cortical GABA interneurons contribute to the neurovascular coupling response to basal forebrain stimulation. *J Cereb Blood Flow Metab*. 2008;28:221–231.
96. Koechlin E, Ody C, Kouneiher F. The architecture of cognitive control in the human prefrontal cortex. *Science*. 2003;302:1181–1185.
97. Gasquoine PG. Contributions of the insula to cognition and emotion. *Neuropsychol Rev*. 2014;24:77–87.
98. Richter-Levin G. The amygdala, the hippocampus, and emotional modulation of memory. *Neuroscientist*. 2004;10:31–39.
99. Opitz B. Memory function and the hippocampus. *Front Neurol Neurosci*. 2014;34:51–59.

100. Fama R, Sullivan EV. Thalamic structures and associated cognitive functions: relations with age and aging. *Neurosci Biobehav Rev*. 2015;54:29–37.
101. Hashimoto T, Arion D, Unger T, et al. Alterations in GABA-related transcriptome in the dorsolateral prefrontal cortex of subjects with schizophrenia. *Mol Psychiatry*. 2008;13:147–161.
102. Yoon JH, Minzenberg MJ, Ursu S, et al. Association of dorsolateral prefrontal cortex dysfunction with disrupted coordinated brain activity in schizophrenia: relationship with impaired cognition, behavioral disorganization, and global function. *Am J Psychiatry*. 2008;165:1006–1014.
103. Wylie KP, Tregellas JR. The role of the insula in schizophrenia. *Schizophr Res*. 2010;123:93–104.
104. Tregellas JR, Smucny J, Harris JG, et al. Intrinsic hippocampal activity as a biomarker for cognition and symptoms in schizophrenia. *Am J Psychiatry*. 2014;171:549–556.
105. Skudlarski P, Jagannathan K, Anderson K, et al. Brain connectivity is not only lower but different in schizophrenia: a combined anatomical and functional approach. *Biol Psychiatry*. 2010;68:61–69.
106. Klingner CM, Langbein K, Dietzek M, et al. Thalamocortical connectivity during resting state in schizophrenia. *Eur Arch Psychiatry Clin Neurosci*. 2014;264:111–119.
107. Byne W, Hazlett EA, Buchsbaum MS, Kemether E. The thalamus and schizophrenia: current status of research. *Acta Neuropathol*. 2009;117:347–368.
108. Pergola G, Selvaggi P, Trizio S, Bertolino A, Blasi G. The role of the thalamus in schizophrenia from a neuroimaging perspective. *Neurosci Biobehav Rev*. 2015;54:57–75.
109. Lindenmayer JP, Harvey PD, Khan A, Kirkpatrick B. Schizophrenia: measurements of psychopathology. *Psychiatr Clin North Am*. 2007;30:339–363.
110. Hirjak D, Wolf RC, Wilder-Smith EP, Kubera KM, Thomann PA. Motor abnormalities and basal ganglia in schizophrenia: evidence from structural magnetic resonance imaging. *Brain Topogr*. 2015;28:135–152.
111. Kaufmann T, Skatun KC, Alnaes D, et al. Disintegration of sensorimotor brain networks in schizophrenia. *Schizophr Bull*. 2015;41:1326–1335.
112. Lee CU, Shenton ME, Salisbury DF, et al. Fusiform gyrus volume reduction in first-episode schizophrenia: a magnetic resonance imaging study. *Arch Gen Psychiatry*. 2002;59:775–781.
113. Onitsuka T, McCarley RW, Kuroki N, et al. Occipital lobe gray matter volume in male patients with chronic schizophrenia: a quantitative MRI study. *Schizophr Res*. 2007;92:197–206.
114. Onitsuka T, Shenton ME, Kasai K, et al. Fusiform gyrus volume reduction and facial recognition in chronic schizophrenia. *Arch Gen Psychiatry*. 2003;60:349–355.
115. Perez-Costas E, Melendez-Ferro M, Roberts RC. Basal ganglia pathology in schizophrenia: dopamine connections and anomalies. *J Neurochem*. 2010;113:287–302.
116. Schultz CC, Wagner G, Koch K, et al. The visual cortex in schizophrenia: alterations of gyrification rather than cortical thickness–a combined cortical shape analysis. *Brain Struct Funct*. 2013;218:51–58.
117. Wang D, Zhou Y, Zhuo C, et al. Altered functional connectivity of the cingulate subregions in schizophrenia. *Transl Psychiatry*. 2015;5:e575.
118. Javitt DC. Sensory processing in schizophrenia: neither simple nor intact. *Schizophr Bull*. 2009;35:1059–1064.
119. Javitt DC, Freedman R. Sensory processing dysfunction in the personal experience and neuronal machinery of schizophrenia. *Am J Psychiatry*. 2015;172:17–31.
120. Walther S, Strik W. Motor symptoms and schizophrenia. *Neuropsychobiology*. 2012;66:77–92.
121. Harvey PD, Lombardi J, Leibman M, et al. Cognitive impairment and negative symptoms in geriatric chronic schizophrenic patients: a follow-up study. *Schizophr Res*. 1996;22:223–231.
122. Antonova E, Sharma T, Morris R, Kumari V. The relationship between brain structure and neurocognition in schizophrenia: a selective review. *Schizophr Res*. 2004;70:117–145.
123. Anderson JE, Wible CG, McCarley RW, Jakab M, Kasai K, Shenton ME. An MRI study of temporal lobe abnormalities and negative symptoms in chronic schizophrenia. *Schizophr Res*. 2002;58:123–134.